Cable Stiffness Characterization for a single layered cable – sheave contact through mathematical model

Rajesh Kumar P[1], *D.* Sriram[2], *Rajan* VR[3], *Chanakyan* C[4], *Ashok* Raj R[5], *H. S.* Manjunath[6], *Prakash* J[7], *Suresh* Kumar S[8], *P.* Ramkumar[9]
[1]Department of Mechanical Engineering, MVJ College of Engineering, Bangalore, India
[2]Department of Mechanical Engineering, Indra Ganesan College of Engineering, Trichy, India
[3] Department of ECE, T. John Institute of Technology, Bangalore, Visvesvaraya Technological University, India
[4]Department of Mechanical Engineering, Global Academy of Technology, Bengaluru, India
[5&7]Department of Mechanical Engineering, J.J. College of Engineering and Technology, Trichy, Tamil Nadu, India
[6]Department of Mechanical Engineering, Dr. Ambedkar Institute of Technology, Bangalore, India
[8]Department of Mechanical Engineering, PERI Institute of Technology, Mannivakkam, Chennai 600048, Tamil Nadu, India
[9]Department of Mechanical Engineering, Kalasalingam Academy of Research and Education, Krishnankoil, Virudhunagar, India

Abstract. The characterization of cable stiffness has gained importance due to the increasing demand for longer cable life cycles. This has spurred research interest in studying the contact mechanics of cable-sheave assemblies to enhance stiffness performance. In this context, the current work to tests one-layered stiffness of helical strand composed of a stretched central core surrounded by six helical wires in core-wire contact. The stranded cable bends uniformly as it passes on a sheave. For static loading conditions, considered for various combined loadings like tension, torsion, and bending. This study employs thin rod theory and linear elasticity to develop a novel mathematical model describing the cable's behavior when in contact with the pulley or sheave. The stiffness values, including axial, torsional, and flexural rigidities, along with coupling parameters, are determined and estimated. Based on these estimations and computational analyses, the effect of the sheave or pulley's deformation on cable stiffness is examined, considering the interplay of tension, torsion, bending, and the contact state with the sheave.

*Corresponding author: prajeshkumarmvjce@gmail.com

1 Introduction

Stranded cables frequently impose some transverse strain or curvature in practical applications, when they are used over sheaves or rollers in material handling or subjected to vibrations, when used as overhead transmission line conductors [1]. They are classified respectively as constrained bending case and free bending case. It is well known that a helical strand in bending has two limiting behaviours viz., Solid or monolithic behaviour and Loose-wire behaviour [3]. In solid behaviour, all the wires in the strand are assumed to act as a single unit. In Loose-wire behaviour, all the wires are assumed to act independently, as if there is no friction in the strand. In reality the cable/strand behaviour lies in between the two extremes and often poses a challenge to evaluate it. The consideration of the proper contact modes, frictional effect and associated slip at the contact interface, will help to evaluate the stiffness of the cable realistically. Although cables have been used for centuries, there are limited and contemporary theoretical models for bending helically wrapped wires. Costello et al. [2] provided a model for cable bending that incorporates twisting but ignores friction and slippage between the wires. In a strand model, Lanteigne et al. [3] included wire bending with the wire axial force. For the identical situation, Knapp et al. [4] calculated wire binormal curvature and twist, but the analysis was limited to wire axial strain. The wire bending and twisting, as well as the wire forces, were considered by LeClair et al. [5], but the final solution was difficult to accept due to the relatively low wire axial force, in their own words. Parthasarathy et al. [6] has accounted for the loss of stiffness of a stranded cable due to the consideration of axial and twist slips at the contact interface. Hobbs et al. [7] used first principles to calculate the bending strain in frictionless rope wires when a rope is bent into a circular arc, the curvature of both single and double helices adjusts accordingly to accommodate the new shape. The friction, on the other hand, was not considered in the study. Sathikh et al. [8] proposed a mathematical expression incorporating wire-to-core contacts to determine the pre-slip bending behavior of a helical wire strand subjected to constant curvature bending, considering unbounded Coulomb friction. Marco Giglio et al. [9] analyzed the stress distribution in the inner and outer wires of a rope bent over a small sheave, considering the changes in curvature between the undeformed and deformed states. This research significantly contributed to the fatigue analysis of wires. Rajesh Kumar et al. [10] [11] discussed about the single layered cable stiffness core wire (radial contact) alone having friction between wire and the core. Ramsey. [15] proposed a theory for a thin rod model to analyse a steel strand with frictional forces in all the contact modes, and observed that the contact forces helped to prevents the wires from their of helix angle changes.. Shankar et al. [12] analysed transmission line conductor for bending deflection under refined slip model. Wokem et al. [13] addressed the cable performance over a sheave. The reliability of the cable dependency on different parameters like strand geometrical construction, sheave specifications and diametrical ratios of cable-sheave was studied. A finite element model was constructed using the experimental specifications of nineteen wires strand and seven wires strand. The stress concentration factor found to increase with load and decreased with increasing cable sheave diametrical ratio. The location of the critical wires seemed to be the wires that are in contact with the sheave. Chuntian Xu et al. [14] propose a model for predicting the transmission error of cable-driven sheaves (CDS) based on their cable deformation, which is derived from the classical Capstan equation and Hooke's law, respectively, without

considering the effects of the friction coefficient between wire strands. To the best of the knowledge no authors have given an adequate treatment over those helical wires in stranded cable in contact with the sheave/pulley and finding the response using the stiffness as coupling coefficients. In this paper an attempt is made to study the bending stiffness of those wires in contact with the sheave/pulley under constant curvature bending considering coupling coefficient, and my work is in consistent with UN sustainability Goal SDG 9- Industry innovations and infrastructure that lead to better engineering designs that improve efficiency of cranes, elevators, cable cars, and power transmission lines. SDG 12- Responsible Consumption and Production by reducing wear and tear, fewer cables need to be manufactured and disposed.

2 Extraction of the model

Each wire in the strand is analyzed as a long, slender curved rod in the following study. The cross-sectional area of a seven-wire cable, the derived geometric relations and the evolved shape of a one helical rod are shown in Figures 1(a), 1 (b) and 1(c) respectively. The strand begins with a stretched core radius (Rc), which is encircled by 'm' number of helical rods with a radius (Rw) and angle of a helix α.

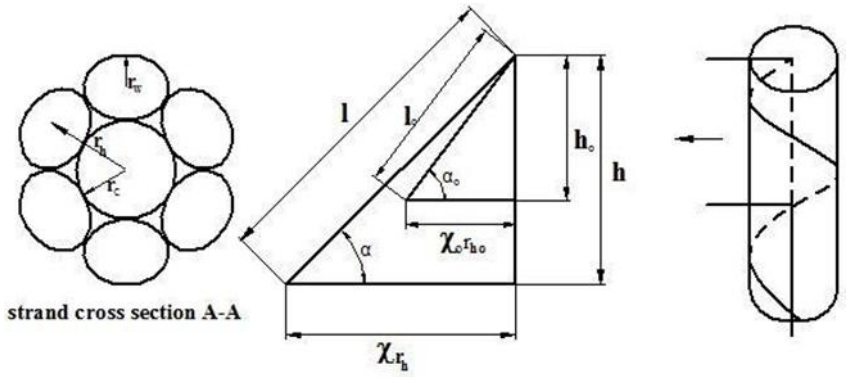

Fig. 1. (a) Strand Cross Section (b) derived geometric relations (c) Evolved Shape of a single helical wire

From Fig.1b shown the relative expressions written as

$h = l \sin\alpha$ (01)
$r_h\chi = l \cos\alpha$ (02)
$\tan\alpha = h/r_h\chi$ (03)

where 'h' is the strand height, and l & r, are the wire length and helix radius, and α & χ, are the angle of helix and the angle of swept of the helical rod.
The following kinematic conditions are adopted for the core and the wire.

$\delta r = 0,\ \ \delta l \neq 0,\ \delta\alpha \neq 0, \delta\chi \neq 0$ (04)

When the deformation is small, the mechanics relations yield for helix radius r_h

$$\delta\alpha = [\delta h \cos\alpha/(r_h) - \sin\alpha\,\delta\chi]/(l/r_h) \quad (05)$$

$$\delta l = [l\cos\alpha\delta\chi + (l/r_h)\sin\alpha\delta h](l/r_h) \quad (06)$$

The wire axial strain can therefore be calculated easily using the cable axial strain ϵ and the stand rotational strain γ, as follows:

$$\epsilon_w = \epsilon\sin^2\alpha + \gamma\cos^2\alpha \quad (07)$$

Further the strand rotational strain can be written as

$$\gamma = \frac{\partial\chi}{\chi} = \frac{\partial\chi}{h} r_h \tan\alpha \quad (08)$$

2.1 Contribution of Stiffness coefficient to the wire tensile strain under pure bending

The contribution of the stiffness coefficient to the axial strain of the wire under pure bending is considered for the mathematical modelling.

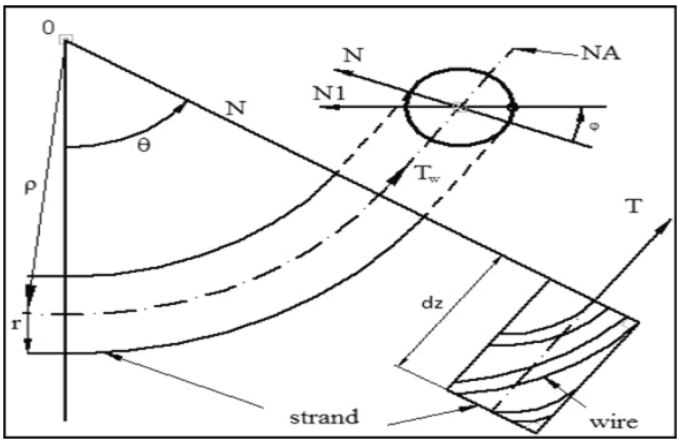

Fig. 2. Geometry of bent strand

From the geometry of bent strand in figure 2, the neutral axis strands elemental length dz remains same after bending. Thus

$$dz = \rho d\theta \quad (09)$$

However, another elemental length dz_1 at a position at a distance $r\cos\phi$ from the neutral axis would vary its length as follows:

$$dz_1 = \rho_1 d\theta = (\rho + r\cos\phi)d\theta \quad (10)$$

The cable tensile strain for ϕ from (9) and (10) is

$$\varepsilon = \frac{dz_1 - dz}{dz} = \frac{\delta z}{dz} = \frac{r\cos\phi}{\rho} \quad (11)$$

And utilising as (21) as the wire axial strain and bi-normal displacement of the wire centre per unit length inclined at angle α obtained as

$$(\varepsilon_{wi}, \gamma_{wi}) = (\sin^2\alpha, \sin\alpha\cos\alpha)\, r\cos\phi/\rho \quad (12)$$

The wire tensile strain ε_w per unit length of wire inclined at α was established as

$$\varepsilon_{w(bending)} = \frac{r\sin^2\alpha\cos\phi}{\rho} \quad (13)$$

Wire combined wire tensile load includes load due to bending

The total tensile strain of the wire can be written as

$$\varepsilon_w = \varepsilon_{w(axial)} + \varepsilon_{w(bending)} \quad (14)$$

Adding equation (07) and (13)

$$\varepsilon_w = sin^2\,\alpha\,\varepsilon + r\,sin\,\alpha\,cos\,\alpha\frac{\delta\chi}{h} + \frac{r\,sin^2\,\alpha\,cos\,\phi}{\rho} \quad (15)$$

2.2 Curvature and Twist of the helical rod

A straight strand, the curvature and twist helical rod (for absence of slip) in the normal, transverse, and tensile directions are expressed as follows.

$$k_0 = 0,\ k'_0 = \frac{cos^2\,\alpha}{r},\ \tau_0 = \frac{sin\,\alpha\,cos\,\alpha}{r} \quad (16)$$

The overall twist and curvature of a helical rod, subjected to the added effects of tensile and bending loads, are determined by

$$k_1 = k_o + \Delta k,\ k = k_o + \Delta k,\ \tau_1 = \tau_o + \Delta\tau \quad (17)$$

Ramsey et al. [26] established the flexural and torsional strains of wires along normal, bi-normal directions, as well as the torsional strain in the tensile direction. Initially derived the generic formulae for curvatures and torsion for wire rotation alone, then extended them to wire rotation with wire stretch [27]. Based on these theories, Sathikh et al. [28] derived expressions for changes in curvature in normal and bi-normal wire directions, and for change in twist about the wire axial direction.

As a result of the aforesaid theories, changes in normal curvature Δk, change in binormal curvature Δk′, and change in twist Δτ can be achieved for a straight strand configuration as.

$$\Delta k = 0;\ \Delta k' = -\frac{sin^2\,\alpha\,cos^2\,\alpha}{r}\epsilon + sin\,\alpha\,cos\,\alpha\,(1 + sin^2\,\alpha)\frac{d\chi}{h};\quad \Delta\tau = \frac{sin\,\alpha\,cos^3\,\alpha}{r}\epsilon + sin^4\,\alpha\frac{d\chi}{h} \quad (18)$$

Further, Sathikh et al. [28] derived expressions for pure bending loading conditions.Therefore, change in curvature and change in flexure of a helical rod subjected to a addition of tenile deflection and strand curvature is observed as per the above theory is given by

$$\Delta K = \frac{sin\,\alpha(1+cos^2\,\alpha)\,sin\,\varphi}{\rho};\quad \Delta K' = \frac{-\,sin^2\,\alpha\,cos^2\,\alpha}{r}\epsilon + sin\,\alpha\,cos\,\alpha(1 + sin^2\,\alpha)\frac{\delta\chi}{h} + \frac{sin^4\,\alpha\,cos\,\varphi}{\rho};\ \Delta\tau = \frac{sin\,\alpha\,cos^3\,\alpha}{r}\epsilon + sin^4\,\alpha\frac{\delta\chi}{h} - \frac{sin^3\,\alpha\,cos\,\alpha cos\,\varphi}{\rho} \quad (19)$$

Constitutive equations

The wire force, bending moment twisting moment in the axial, normal, binormal and along the axis of the wire direction can be given by

$$T = EA\boldsymbol{\epsilon_w}\quad G = EI\Delta k \qquad G' = EI\Delta k' \qquad H = C\mathcal{J}\Delta\tau \quad (20)$$

2.3 Forces and Moments in the twisted Wire

In all the three directions, components of stress resultants acting on the cross section of the wire are designated by T, N, N', while components of moment acting on the cross section of the wire are denoted by H, G, G'. In normal bi-normal and axial directions, the spread loads per unit length of the rod have components X, Y, and Z, along with the parts of the distributed moments operating per length of the rods like K, K', as illustrated using Figure 3.

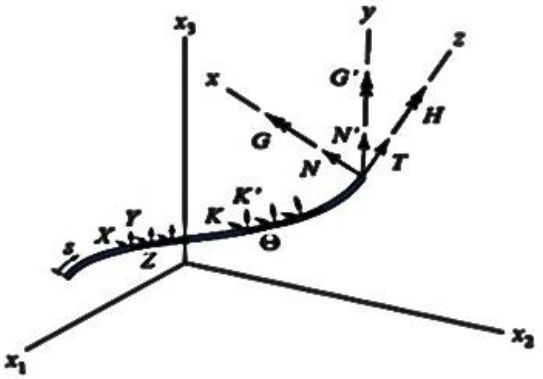

Fig. 3. Different types of loads on helical wires

Using the expressions of the helical rod the shear loads in the normal, transverse directions are given by

N=-$G\tau_o$ **(**21)

$$N' = Hk_0' - G'\tau_0 \quad (22)$$

2.4 Sheave contact

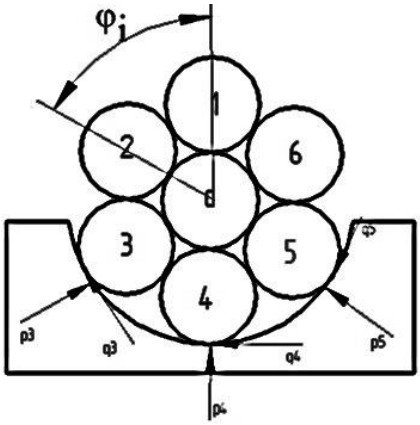

Fig. 4. Wires in contact with the sheave

When the cable runs over pulley/sheave the cable maintains a constant radius of curvature as in figure 4. The U-grooved pulley is considered for the present construction. Under any instant three wires of six helical wires in the inner layer only establishes contact with the pulley. Unlike the other three wires which are not in contact with the pulley these three wire gains contact with the pulley which are at $\boldsymbol{\varphi = 120°,\ \varphi = 180°,\ \varphi = 240°}$ position angles from vertical reference experiences an additional forces about the normal and bi-normal directions exerted by the pulley. These forces are referred as line loads per unit length in the present formulation. So, the three wires at any instant loose connection with the sheave considered as free bending while, other three wires gain pulley contact considered as a constrained bending in the global stiffness of a stand. while additional contact forces which is developed at any instant on the three wires at the inner layer of the stranded cable, when passes over the pulley is shown in figure 4. Let the spread force per unit length along the radial direction that the pulley produced over the contacting wire, this force is acting about the normal direction and also in connection the coefficient of friction 'μ' at the junction of cable and pulley, produces friction load 'μp' that alters the wire tension. Let p3, p4 and p5 be the radial force exerted on the wire3, wire4 and wire5, having position angles$\boldsymbol{\varphi = 120°, \varphi = 180°, \varphi = 240°}$. And p3=p4=p5=p that is all the forces have the same intensities acting in the normal direction to their respective wires. And all these forces are in connection with frictional coefficient 'μ' between the cable and sheave, leads to a friction force 'μp3', 'μp4' and 'μp5' which modifies the wire tension as:

$$\mathrm{T_{\Sigma 3wire}} = \mathrm{EA}\sin^2\alpha\,\varepsilon + \mathrm{EAr}\sin\alpha\cos\alpha\frac{\delta\chi}{\mathrm{h}} + \frac{\mathrm{EAr}\sin^2\alpha\cos\varphi}{\rho} + \mu\mathrm{p3}\rho + \mu\mathrm{p4}\rho + \mu\mathrm{p5}\rho \quad (23)$$

Let q be the force produced by the sheave over the contact wires, this load is also the one-dimensional load per unit length along bi-normal direction. This force couples with bi-normal shear force of contacting wire.
Let q3, q4 and q5 be the radial force exerted on the wire3, wire4 and wire5, having position angles$\boldsymbol{\varphi = 120°, \varphi = 180°, \varphi = 240°}$. And q3=q4=q5=q that is all the forces have the same intensities acting in the bi-normal direction to their respective wire which modifies the wire shear force as:

$$N'_{\Sigma 3wire} = Hk_0' - G'\tau_0 + q3 + q4 + q5 \quad (24)$$

2.5 Equilibrium equation of the stranded cable

The overall cable tensile force, twisting and bending moment, have their helical wire components from (19) to (33). The resultant forces and moments including core deformation is given by.

$$F_a = E_cA_c + (m-3)(T\sin\alpha + \mathrm{N'}\cos\alpha) + T_{\Sigma 3wire}\sin\alpha + \mathrm{N'_{\Sigma 3wire}}\cos\alpha \quad (25)$$

$$M_t = G_c J_c + (m-3)(H\sin\alpha + G'\cos\alpha + Tr\cos\alpha - N'r\sin\alpha) + (H\sin\alpha + G'\cos\alpha + T_{\Sigma 3wire} r \sin\alpha - N'_{\Sigma 3wire} r\cos\alpha) \quad (26)$$

$$M_b = E_c I_c + (m-3)[(T\sin\alpha + N'\cos\alpha)r\cos\varphi + G\sin\varphi + G'\sin\alpha\cos\varphi - H\cos\alpha\cos\varphi - N\,r\cot\alpha\sin\varphi]) + [(T_{\Sigma 3wire}\sin\alpha + N'_{\Sigma 3wire}\cos\alpha)r\cos\varphi + G\sin\varphi + G'\sin\alpha\cos\varphi - H\cos\alpha\cos\varphi - N\,r\cot\alpha\sin\varphi] \quad (27)$$

2.6 Stiffness of the stranded Cable

The stranded cable global stiffness parameters can be derived by using the stiffness matrix, by relating to the global strand loads to deformations as,

$$\begin{Bmatrix} \boldsymbol{F}_a \\ \boldsymbol{M_t} \\ \boldsymbol{M_b} \end{Bmatrix} = \begin{bmatrix} K_{aa} & K_{at} & K_{ab} \\ K_{ta} & K_{tt} & K_{bt} \\ K_{ba} & K_{bt} & K_{bb} \end{bmatrix} \begin{Bmatrix} \varepsilon \\ \delta\chi/h \\ 1/\rho \end{Bmatrix} \quad (28)$$

where ϵ, $\delta\chi/h$ and $1/\rho$ are the cable tensile strain, twist per unit length and curvature respectively. K_{aa}, K_{tt} and K_{bb} are cable tensile stiffness, cable torsional and flexural rigidities. K_{at}andK_{ta} are axial-twist, K_{ab} and K_{ba} are the axial-bending. K_{bt}andK_{tb} are the tension bending connecting entities, for a free bending case. Like wise the stiffness matrix for constrained bending can be derived. The stiffness coefficients were derived for core and three outer wires which will be treated as pure bending and three wire in touch with the sheave considered as constrained bending. The global stiffness of the strand assembly is given in (40)

$$\begin{Bmatrix} \boldsymbol{F}_{\mathrm{a}} \\ \boldsymbol{M}_{t} \\ \boldsymbol{M}_{b} \end{Bmatrix} = \left[\begin{pmatrix} K_{aa(3\,wires+core)} & K_{at(3\,wires)} & K_{ab(3\,wires)} \\ K_{ta(3\,wires)} & K_{tt(3\,wires+core)} & K_{bt(3\,wires)} \\ K_{ba(3\,wires)} & K_{bt(3\,wires)} & K_{bb(3\,wires+core)} \end{pmatrix} + \begin{pmatrix} K_{aa\left(\Sigma(wire(3)+wire(4)+wire(5))\right)} & K_{at\left(\Sigma(wire(3)+wire(4)+wire(5))\right)} & K_{ab\left(\Sigma(wire(3)+wire(4)+wire(5))\right)} \\ K_{ta\left(\Sigma(wire(3)+wire(4)+wire(5))\right)} & K_{tt\left(\Sigma(wire(3)+wire(4)+wire(5))\right)} & K_{tb\left(\Sigma(wire(3)+wire(4)+wire(5))\right)} \\ K_{ba\left(\Sigma(wire(3)+wire(4)+wire(5))\right)} & K_{bt\left(\Sigma(wire(3)+wire(4)+wire(5))\right)} & K_{bb\left(\Sigma(wire(3)+wire(4)+wire(5))\right)} \end{pmatrix} \right] \begin{Bmatrix} \varepsilon \\ \delta\chi/h \\ 1/\rho \end{Bmatrix} \tag{29}$$

3. Results and Discussion

To predict the cable response, the geometrical parameters are considered from the experimental sample for Galvanized Iron as shown in Table 1. The experimental datasets are derived from the research works of Shankar G et al., (2018). They have carried research on the experimental evaluation of the bending deflection of the conductor cables. The baseline model selected are tested and validated by simulation for checking the deflection and bending stiffness changing over the length of cable, which is like the objectives of the present work.

Table 1. Specifications of Galvanized Iron

Particulars	**Symbols**	**Values**
Number of helical wires	m	6
Core radius	R_c	3.2mm
Twisted rod radius	R_w	3.15mm
Angle of helix	α	83º
Modulus of elasticity for core and wire	E_c&E_w	210000N/mm^2
Poisson's ratio	í	0.3
Friction coefficient of core-wire	$\boldsymbol{\mu_{c-w}}$	0.5
Frictional coefficient Between sheave-wire	$\boldsymbol{\mu_{s-w}}$	0.5
Radius of curvature	$\boldsymbol{\rho}$	120mm
Strand helical wire position angle	ϕ	0º - 360º

In the present work, the bending response are predicted for a stranded cable passing over the U-grooved sheave. The curvature, twist, the force and moment relations are formulated with basic laws of physics and mechanics. The helical wire shear loads along the normal and transverse directions are derived by using wire equilibrium equations from (26) to (31). The analytical prediction is also compared with the model developed by LeClair and Costello (1988): A free bending describing the cable under combined tension, torsion and bending, the wire centerline is assumed to take deformed helix shape. The analytical predictions of cable stranded stiffness coefficients for constrained and free bending are compared as shown in the table 2. The wire individual contributions and relative significance for the both the models are compared under free bending case as shown in Table 3a, 3b,3c. While comparing the stiffness coefficient for the free bending case, the torsional rigidity shows a significant amount of variation around 68%. This is due to the fact that LeClair and Costello (1988) inadequately considered the wire twist and wire bending effect can be noticed from the Table 3b also there is asymmetry between the coupling parameters in the LeClair and Costello model which is due to omission of wire stretch effect. The present model considers wire twist and wire bending effect along with wire stretch effect.

The remaining stiffness coefficient except torsional rigidity, the percentage of variation is within 2% due to the combined effect of shear force, twist and bending of the wire. Table 2 also gives the stranded cable stiffness coefficient for the present model extended to the constrained bending which is unique in this study where the literature did not address any of the models. An attempt is made to improve the present model of a free bending case. The constrained bending analysis carried out cumulatively in two different stages: as the cable passes through the sheave/pulley at any instant only three wires makes contact with the U-grooved sheave/pulley which are at position angles $\boldsymbol{\varphi = 120°, \varphi = 180°, \varphi = 240°}$:

(a) in the first stage only fourth wire whose position $\boldsymbol{\varphi = 180°}$considered to be in contact with the sheave/pulley.(b) in the successive stage all the three wire are considered to be in contact with sheave/pulley. The analytical predictions for the both the stages were carried out separately in accordance with the conditions as shown in the table 2.

Under unconstrained bending for both the models the bending stiffness coefficients on summation for all the wires for all the positions angles tends to nullify each other and becomes zero. Whereas when the model extended for constrained bending, asymmetry is created among the bending stiffness coefficients this is due to the inclusion of the line loads per unit length in normal and bi-normal directions on the wires contacting the U-grooved sheave. So, while summing up the wire components do not nullify each other and non-zero values are obtained. The axial stiffness of the cable drastically increased around 30% for the constrained model considering only fourth wire in contact with the sheave/pulley, whereas while considering all the three third fourth and fifth wires in contact with the sheave/pulley the axial stiffness further increased around 39% comparing from single contact. Overall increase in axial stiffness for extending the model from free bending to constrained bending considering all the three wires in contact with the sheave/pulley the percentage of increase is around 57%.

Table 2. Correlations of stiffness coefficient for unconstrained and constrained bending

Stiffness coefficient	LeClair (1988) free bending	Present Model		
		Free bending	Considering 4th wire in contact with the sheave	Considering 3rd ,4th& 5th wires in contact with the sheave
k_{aa} (N)	112,90,561	112,90,432	162,22,229	260,85,823
k_{at} (N − mm)	37,36,273	37,38,814	43,55,270	55,88,183
k_{ab} (N − mm)	0	0	-50,06,199	-100,12,397
k_{ta} (N − mm)	37,29,433	37,38,814	49,71,608	74,37,197
k_{tt}(N − mm^2)	22,88,021	70,89,637	81,29,398	102,08,920
k_{tb}(N − mm^2)	0	0	-18,83,064	-37,66,128
k_{ba} (N − mm)	0	0	-102,96,134	-205,51,746
k_{bt}(N − mm^2)	0	0	-19,57,248	-39,14,497
k_{bb}(N − mm^2)	608,98,541	609,00,246	767,94,927	847,42,267

Table 3a. Individual wire contributions and their relative significance compared for present model and LeClair and Costello model for axial component of free bending case

Model	F_ε(N)			F_ϕ(N − mm)			F_γ(N − mm)		
	Wire stretch	Wire twist	Wire bending	Wire stretch	Wire twist	Wire bending	Wire stretch	Wire twist	Wire bending
1	1600230	0.251836	21.71570	623835	431.9471	-1131.52	2540365	-26.518	0
2	1600230	0	43.43141	623835	0	-1123.06	2540365	-26.918	0

Table 3b. Individual wire contributions and their relative significance compared for present model and LeClair and Costello model for twisting component of free bending case

Mode 1	$M_\varepsilon(N-mm)$			$M_\phi(N-mm^2)$			$M_\gamma(N-mm^2)$		
	Wire stretch	Wire twist	Wire bending	Wire stretch	Wire twist	Wire bending	Wire stretch	Wire twist	Wire bending
1	623835	431.9471	-1131.52	243196.5	740871.7	58959.90	990338.4	-45483.8	0
2	623835	0	-2263.05	243196.5	0	-437.815	990338.4	-46169.5	0

Table 3c. Individual wire contributions and their relative significance compared for present model and LeClair and Costello model for bending component of free bending case

Mode 1	$B_\varepsilon(N-mm)$			$B_\phi(N-mm^2)$			$B_\gamma(N-mm^2)$		
	Wire stretch	Wire twist	Wire bending	Wire stretch	Wire twist	Wire bending	Wire stretch	Wire twist	Wire bending
1	2540365	-26.5182	0	990338	-45483.8	0	4032829	2792.354	6001896
2	2540365	0	0	990338	0	0	4032829	2834.452	5999906

Note: Table 3a, 3b, 3c, Model 1 represents present model for free bending case; Model 2 represents LeClair& Costello (1988) model for free bending case

Table 4. Comparing wire strain for the helical wire in the 3rd& 5thposition with experimental values

Force N	Experimental Strain	Present model With three wire contact	Present model With single wire contact	Present model with pure bending	LeClair & Costello model with free bending
0	0.00000000	0.00000000	0.00000000	0.00000000	0.00000000
4000	-0.00969100	-0.00973058	-0.01025629	-0.01268366	-0.01268367
8000	-0.00945600	-0.00957952	-0.01001338	-0.01233464	-0.01233465
12000	-0.00938400	-0.00942846	-0.00977046	-0.01198562	-0.01198564
16000	-0.00916800	-0.00927740	-0.00952755	-0.01163660	-0.01163662
20000	-0.00901800	-0.00912633	-0.00928464	-0.01128758	-0.01128760

Table 5. Comparing wire strain for the helical wire in the 4th position with experimental values

Force N	Experimental Strain	Present model With three wire contact	Present model With single wire contact	Present model with pure bending	LeClair& Costello model with free bending
0	0.00000000	0.00000000	0.00000000	0.00000000	0.00000000
4000	-0.00969100	-0.00973058	-0.01025629	-0.01268366	-0.01268367
8000	-0.00945600	-0.00957952	-0.01001338	-0.01233464	-0.01233465
12000	-0.00938400	-0.00942846	-0.00977046	-0.01198562	-0.01198564
16000	-0.00916800	-0.00927740	-0.00952755	-0.01163660	-0.01163662
20000	-0.00901800	-0.00912633	-0.00928464	-0.01128758	-0.01128760

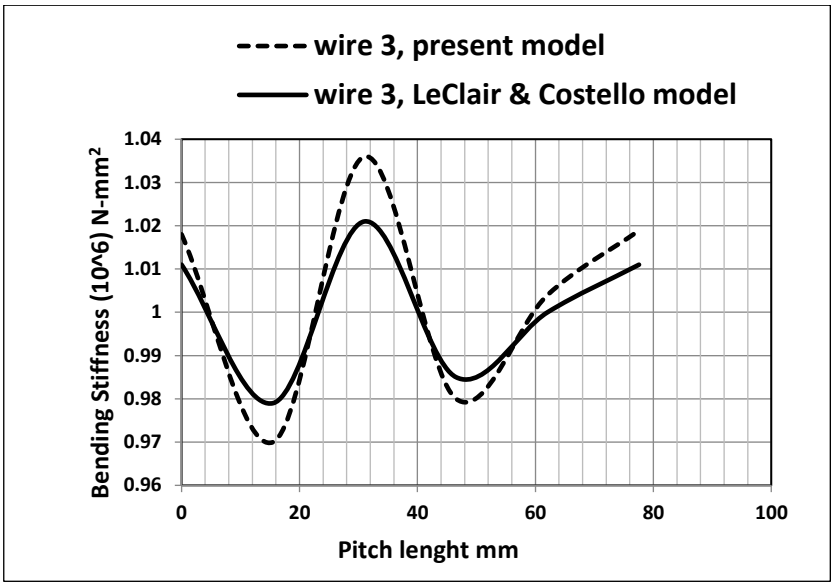

Fig. 5. Bending stiffness for wire 3 contact with the sheave compared for present model with LeClair & Costello of free bending

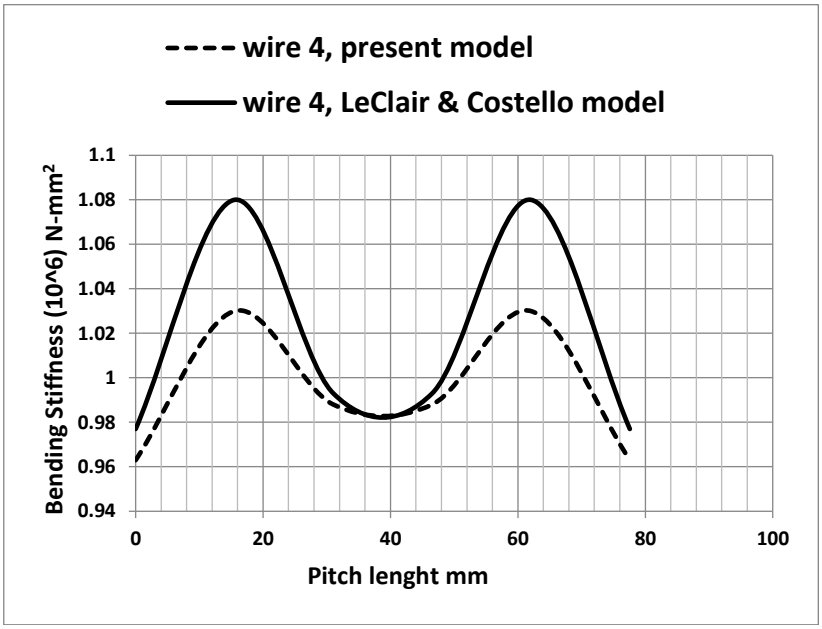

Fig. 6. Bending stiffness for wire 4 contact with the sheave compared for present model with LeClair& Costello of free bending

The bending stiffness Kbb from the table 2 for constrained bending considering only fourth wire in contact with the sheave/pulley for the model extending from free bending exhibits an increase in 21% in comparison with the base model. For model considering all the three, viz., the third fourth and fifth wires in touch with the sheave, the percentage of increase in bending

stiffness is around 9% in comparison with the single contact. In general, there is a significant increase in bending stiffness for all three wires making contacts with the sheave/pulley. Among the coupling stiffness parameters there broke symmetry due to inclusion of shear line per unit length about normal and bi-normal direction and percentage of in stiffness value for Kat & Kta is around 33% & 50%, the other stiffness parameters Kab, Ktb, Kba and Kbt exhibits a non-zero negative value for the constrained model extended from free bending considering all the three wire in contact with the sheave/pulley. The model evolved for the stiffness is in close correlation with the findings of the treated slip expressions for different bending stiffness in a one layered strand developed by Shankar G et al. (2018).

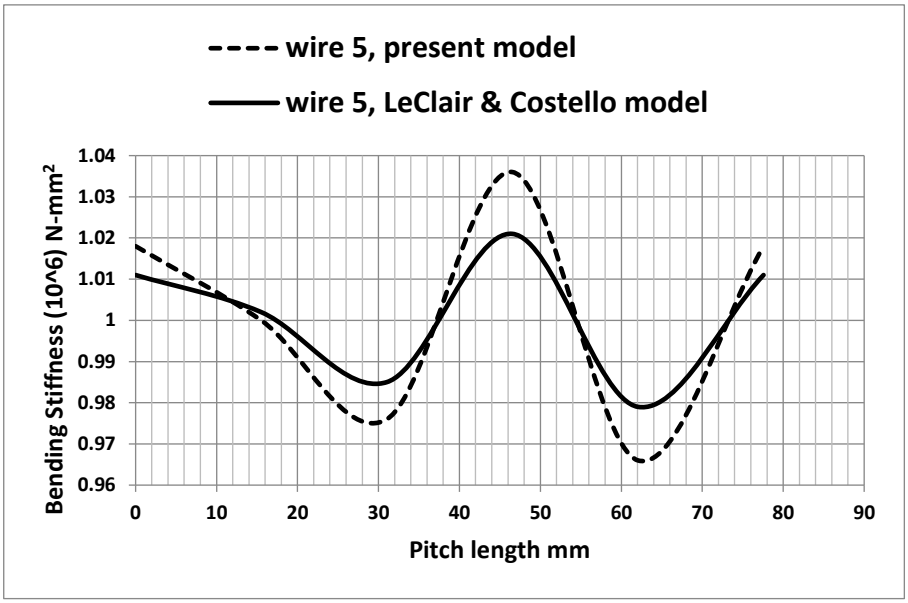

Fig. 7. Bending stiffness for wire5 contact with the sheave compared for present model with LeClair& Costello of free bending

From the Table 3c the wire bending component of bending stiffness for the both the present model and LeClair& Costello model under free bending case the analytical prediction are plotted for the third, fourth and fifth wires and shown in figures 5, 6 and 7. In all the three cases there is an increase in the amplitude for the present model compared with LeClair and Costello model which is due to inclusion of wire stretch effect in the present model for all the three wires whose position angles$\boldsymbol{\varphi = 120°, \varphi = 180°, \varphi = 240°}$.

The wire bending component of bending stiffness for the both the present model for free bending case, considering single contact and three contact with the sheave/pulley and LeClair& Costello model under free bending case the analytical predictions are shown in the table 4 for third and fifth wires and table 5 for fourth wire. It can be observed that as contact is made from free bending to constrained bending the analytical prediction approaches close towards the experimental results.

4. Conclusion

From the critical inferences of the results of the present model constructed for six helical wires surrounding a straight core having core-wire contact mode. The new model was analysed for free bending case which includes wire twist, wire bending and wire stretch effect. The present new model was compared with the LeClair and Costello (1998) model under free bending who is well known author in this field. The analytical predictions carried out exhibit a very close correlation with the actual values. The coupling parameters exhibits symmetry in the present model, which is lacking in the LeClair and Costello model, this is due to the inclusion of wire stretch effect in the present model. And the torsional rigidity Ktt, there is increase of around 68% in the present model, this is due to the inclusion of wire twists and wire bending effect in the present model. The results depict that for the free bending case of both the models, there is increase in the amplitude level for wire bending component for the three wires in the inner layer that contact the sheave/pulley. The free bending model evolved in the present work is further extended to constrain bending which is unique. Cable analysis of constrained bending is carried out cumulatively in two different stages as the cable passes through the sheave/pulley at any instant, only three wires makes contact with the U-grooved sheave/pulley which are at position angles $\boldsymbol{\varphi = 120°, \varphi = 180°, \varphi = 240°}$, viz., (a) in the first stage only fourth wire whose position $\boldsymbol{\varphi = 180°}$ are considered to be in contact with the sheave/pulley, (b) in the successive stage all the three wire are considered to be in contact with sheave/pulley. The analytical predictions for the both the stages were carried out seperately. In the first stage the axial stiffness increases by around 37% and by 57% for the second stage, the bending stiffness increases by around 9% and 21% in the first and second stage in comparison with the free bending of the present model respectively. Further, the results in table 4 and 5, the three wires which makes contact with the sheave/pulley are transformed from free bending to constrained bending, and the analytical prediction approaches close towards the experimental results thereby validating the present mathematical model which has been evolved considering all the forces and moments appropriately. Therefore, this model will provide a mathematical base for the cable designers to accurately predict the stresses/ strains in the wires and to recommend safe operating loads and suitable cable-pulley geometrical combinations.

References

1. H. Shao, D. Li , Z. Kan, L. Bi, Z. Yao, J. Xiang, Numerical simulation of aircraft arresting process with an efficient full-scale rigid-flexible coupling dynamic model. Chi. J. Aero. **37,** 586–602 (2024). https://doi.org/10.1016/J.CJA.2024.03.002
2. G.-A. Costello, G.-J. Butson, Simplified bending theory for wire rope, J. Engg. Mech. 108, 2 (1982). https://doi.org/10.1061/JMCEA3.0002807
3. J. Lanteigne, Theoretical Estimation of the Response of Helically Armored Cables to Tension, Torsion, and Bending. J. Appl. Mech. Jun. **52,** 423-432 (1985). https://doi.org/10.1115/1.3169064
4. R.-H. Knapp, Helical Wire Stresses in Bent Cables. ASME. J. Offshore Mech. Arct. Eng. **110,** 55–61 (1988). https://doi.org/10.1115/1.3257124
5. R.-A. LeClair, G.-A. Costello, Axial, Bending and Torsional Loading of a Strand With Friction. ASME. J. Offshore. Mech. Arct. Eng. **110**, 38–42 (1988). https://doi.org/10.1115/1.3257121
6. N.-S. Parthasarathy, S. Sathikh, Reduced Bending Stiffness and Slip Damping of a Stranded Cable Structure. In ING/IABSE International Seminar on Cable Stayed Bridges, Bangalore, India, (1988).

7. R.-E. Hobbs, S. Nabijou Changes in wire curvature as a wire rope is bent over a sheave. The J Str Ana Engg Design. **30**, 271-281 (1995). doi:10.1243/03093247V304271
8. S. Sathikh, S. Rajasekaran, C.-V. Jayakumar, C. Jebaraj, General thin rod model for pre-slip bending response of strand. J. Engg. Mechan. **126**, 110-11 (2000). https://doi.org/10.1061/(ASCE)0733-9399(2000)126:2(132)
9. M. Giglio, A. Manes, Life prediction of a wire rope subjected to axial and bending loads. Engg. Fail. Anal. **12**, 549–568 (2005). https://doi.org/10.1016/J.ENGFAILANAL.2004.09.002
10. P. Rajesh Kumar, N.-S. Parthasarathy, Stiffness of a Single Layered Cable Assembly over a Sheave with Internal Friction, In.t J. Mech. Engg. Technol. **9**,156–168 (2018). http://iaeme.com/Home/issue/IJMET?Volume=9&Issue=4
11. P. Rajesh Kumar, N.-S. Parthasarathy, Constrained Bending Phenomenon of A Single Layered Cable Assembly. Int. J. Adv. Res. Engg. Technol. **9**, 58-67 (2018)
12. G. Shankar, N.-S. Parthasarathy, Numerical Simulation and experimental Evaluation of Bending deflection of Transmission Line Conductor, Int. J. Adv. Res. Engg. Technol. **9**, 120–128 (2018). http://iaeme.com/Home/issue/IJARET?Volume=9&Issue=6
13. C. Wokem, T.-G. Joseph M Curley, Fatigue prediction for hoist cables over sheaves in large mining shovel application. Fatig. Frac. Engg. Mat. Struc. (2018). https://doi.org/10.1111/ffe.12826
14. X. Chuntian, Li. Jianguang, W. Peng, X. Zhengdong, A Study of Transmission Error Modeling and Preload Compensation for the Cable-Driven Sheaves Used in Space Docking Locks. J. Mecha. **36**, N9–N20 (2020). https://doi.org/10.1017/jmech.2020.41
15. H. Ramsey, A theory of thin rods with application to helical constituent wires in cables. Int. J. Mecha. Sci. **30**, 559–570 (1988). https://doi.org/10.1016/0020-7403(88)90099-9